

Strong-Field Photoionization as Excited-State Tunneling

E. E. Serebryannikov and A. M. Zheltikov*

Physics Department, International Laser Center, M. V. Lomonosov Moscow State University, Moscow 119992, Russia

Department of Physics and Astronomy, Texas A&M University, College Station, Texas 77843-4242, USA

Russian Quantum Center, ul. Novaya 100, Skolkovo, Moscow Region 143025, Russia

(Received 5 April 2015; published 24 March 2016)

We show that, in an intense laser field, ultrafast photoionization can occur through quantum pathways that cannot be categorized as multiphoton ionization or ground-state tunneling. In this regime, the subcycle electron-wave-packet dynamics leading to photoionization occurs via electron excited states, from where the electrons tunnel to the continuum within a tiny fraction of the field cycle. For high field intensities, this ionization pathway is shown to drastically enhance the dynamic leakage of the electron wave packet into the continuum, opening an ionization channel that dominates over ground-state electron tunneling.

DOI: 10.1103/PhysRevLett.116.123901

Field-induced ionization is one of the key effects in strong-field laser-matter interactions. In a broadly accepted intuitively appealing model, photoionization is viewed as a result of direct electron transitions from the electron ground state to the continuum [1–5]. As shown in the seminal work by Keldysh [1], this model gives a convenient closed-form expression for the photoionization rate, providing a universal framework for the description of both multiphoton and tunneling regimes of photoionization [Fig. 1(a)] and offering a powerful tool for practical calculations. Over almost five decades, this model, originally intended for continuous-wave fields [1], has been pivotal to ultrafast laser science, providing a universal framework for a quantitative analysis of ionization in a remarkable diversity of phenomena, including laser-induced breakdown [6,7] and high-order harmonic [8,9] and terahertz [10–12] generation, as well as filamentation of ultrashort light pulses [13,14].

However, as rapidly progressing laser technologies enable the generation of extremely short high-intensity optical waveforms [15,16], allowing time-resolved studies on an unprecedentedly short time scale [17–22], photoionization theories need to explain the details of field-induced ionization dynamics within the field cycle. Several approaches have been developed to address this problem. In the context of high-order harmonic generation, Lewenstein *et al.* [2] have developed an instructive path-integral approach to the analysis of tunneling electron trajectories in the presence of a high-intensity ultrashort driving pulse. Ammosov, Delone, and Krainov [5], as well as Yudin and Ivanov [23], have derived physically insightful closed-form cycle-averaging-free procedures for an approximate analysis of electron tunneling on the subcycle time scale. These single-bound-state theories of photoionization help identify new field-cycle-sensitive phenomena in electron tunneling [17,24,25] and develop novel experimental methods for all-optical detection of electron tunneling dynamics [26,27].

A fundamental issue that remains unresolved in these theories is related to the role of excited electron bound states in ultrafast photoionization dynamics. In experiments

with many-cycle laser pulses, electron bound states show up as resonant features in the spectra of photoelectrons [28,29] and nonlinear-optical signals [30]. As the driver pulse width becomes shorter, approaching the field cycle, these features become less pronounced [31]. However, electron bound states, as we will show below in this work, continue to play a significant role, enhancing nonlinear-optical interactions. While the experimental work spanning over three decades [28–30,32] provides strong evidence for the significance of excited-state dynamics for nonlinear optics in fast-ionizing media, most of the photoionization theories include only one (most of the time, ground) bound electronic state, treating photoionization as a transition of an electron from this bound state to the continuum.

As we show below in this Letter, the dynamic description of field-induced ionization on the ultrafast time scale is incomplete unless the dynamics of electron excited states is included in the model. We demonstrate that, for extremely short and intense laser pulses, photoionization can no longer be categorized into a multiphoton process and

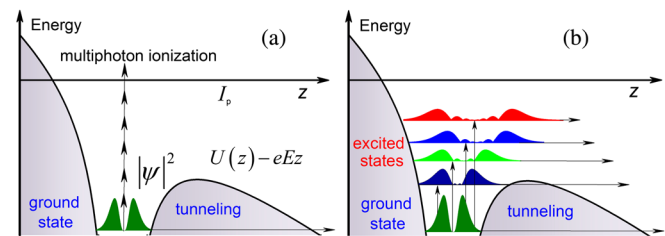


FIG. 1. Laser-induced ionization: (a) multiphoton and tunneling ionization in a standard model of photoionization including only one bound state and (b) photoionization through tunneling from excited states. The attractive potential of the atomic core, $U(z)$, is modified by the laser field E , giving rise to a potential barrier $U(z) - eEz$ of finite width. The electron wave function $\psi(z)$ can now leak through this barrier. Excited bound states open additional pathways for this tunneling process. The $|\psi(z)|^2$ profiles are shown in different colors. Vertical arrows show transitions coupling the ground state to excited states and the continuum.

ground-state tunneling [Fig. 1(a)]. Instead, the subcycle electron-wave-packet dynamics leading to photoionization occurs via electron excited states, from where the electrons tunnel to the continuum within a tiny fraction of the field cycle [Fig. 1(b)]. For high field intensities, this ionization pathway is shown to dominate over the tunneling of ground-state electrons.

Our analysis of photoionization is based on the time-dependent Schrödinger equation (TDSE) for the wave function $\psi(\vec{r}, t)$ (\vec{r} is the radial coordinate and t is the time) in the presence of a driver field, which is assumed to be linearly polarized along the z axis and have a Gaussian envelope $E(t) = E_0 \exp(-t^2/\tau^2) \cos(\omega_0 t)$. The TDSE is solved on a spatial grid using a modified fourth-order Crank-Nicholson propagator [33]. At the initial moment of time, the quantum system is assumed to be in the $1s$ ground state of a hydrogen atom. The driver pulse width is set equal to $\tau = 10/\omega_0$.

We represent the length-gauge solution to the TDSE as a sum

$$\begin{aligned} \psi(\vec{r}, t) &= \psi_b(\vec{r}, t) + \psi_f(\vec{r}, t) \\ &= \sum_{n=1}^N \sum_{l=0}^{n-1} \alpha_{n,l}(t) \psi_{n,l}(\vec{r}) + \psi_f(\vec{r}, t) \end{aligned} \quad (1)$$

of negative- and positive-energy terms, $\psi_b(\vec{r}, t)$ and $\psi_f(\vec{r}, t)$, corresponding to the bound and free (continuum) states of an electron [34,35], respectively, with $\psi_{n,l}(\vec{r})$ being the orthonormalized eigenfunctions of the stationary Schrödinger equation for a hydrogen atom.

The probability to find an electron in a bound state with quantum numbers n and l is then given by $|\alpha_{n,l}(t)|^2 = |\int_V \psi_{n,l}(\vec{r}) \psi(\vec{r}, t) d\vec{r}|^2$. The ionization probability, that is, the probability to find an electron in the continuum, referred to hereinafter as the continuum population, at the instant of time t is found as $C(t) = \int_V |\psi_f(\vec{r}, t)|^2 d\vec{r}$.

As everyone's gold standard for a single-bound-state model of photoionization, we use the Keldysh length-gauge formulation of strong-field approximation (SFA), treating photoionization as a direct transition of a ground-state electron with charge e to a Volkov-type continuum state (see, e.g., canonical texts of Refs. [1–5,36,37] for a review). Such an approach gives

$$\begin{aligned} C(t) &= \int |a_p(t)|^2 d\vec{p} \\ &= \int \left| -\frac{i}{\hbar} \int_{-\infty}^t \left(\int_V \psi_p^*(\vec{r}, t') eE(t') z \psi_i(\vec{r}, t') d\vec{r} \right) dt' \right|^2 d\vec{p}, \end{aligned} \quad (2)$$

where $\psi_i(\vec{r}, t) = \psi_0(\vec{r}, t) = \psi_0(\vec{r}) \exp(iI_p t/\hbar)$, $\psi_0(\vec{r})$ is the wave function of the initial state, I_p is the ionization potential, and $\psi_p(\vec{r}, t) = (2\pi)^{-3/2} \exp\{i[(\vec{\pi} \cdot \vec{r}) -$

$\int_0^t |\vec{\pi}|^2/2m_e d\tau]/\hbar\}$ is the Volkov wave function with $\vec{\pi}(t) = \vec{p} - e \int_{-\infty}^t E(t') dt'$.

Figures 2(a)–2(c) present the buildup of the continuum population $C(t)$ induced by an ultrashort laser driver calculated with the use of the TDSE and the standard, single-bound-state SFA model of Eq. (2) for different intensities I_0 of the driver field. In Figs. 2(d) and 2(e), we compare TDSE simulations with the predictions of Eq. (2) for the continuum population in the wake of the driver pulse. For low peak intensities I_0 of the driver field [$I_0 < 1$ TW/cm²], the single-bound-state SFA model, as can be seen from Figs. 2(a) and 2(d), agrees very well with TDSE simulations. However, for high field intensities [starting with approximately 1 TW/cm²], the single-bound-state SFA model is seen to systematically underestimate the continuum population [Figs. 2(b), 2(c), and 2(e)]. Specifically, in the range of

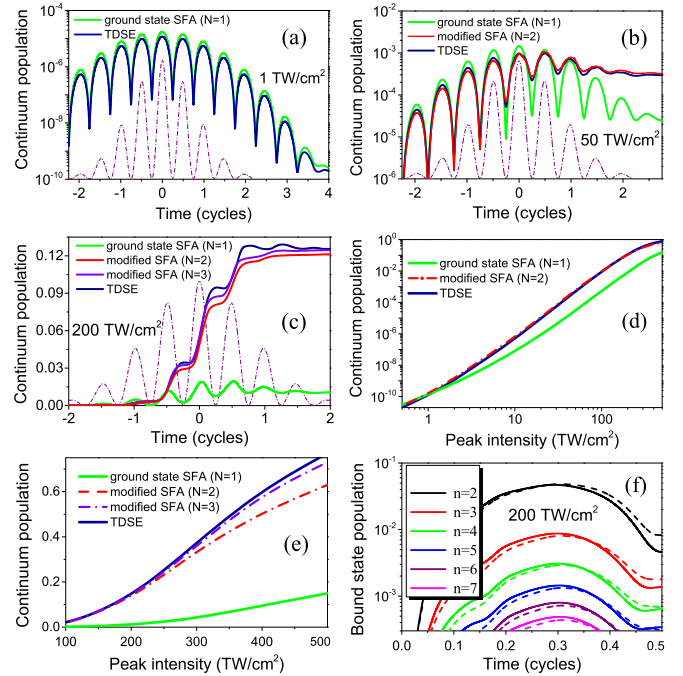


FIG. 2. (a)–(c) Continuum population buildup induced by an ultrashort driver pulse (shown by the dash-dotted line) with the central wavelength with $\lambda_0 = 0.8 \mu\text{m}$ and peak intensity $I_0 = 1$ (a), 50 (b), and 200 TW/cm² (c) calculated through a numerical solution of the TDSE (blue line) and by using the standard, single-bound-state SFA model of Eq. (3) (green line) and modified SFA of Eqs. (4) and (5) with $N = 2$ (red line) and $N = 3$ (violet line). (d), (e) Continuum population as a function of the peak intensity of the pulse driver calculated through a numerical solution of the TDSE (blue line) and by using the standard SFA model of Eq. (3) (green line) and modified SFA of Eqs. (4) and (5) with $N = 2$ (red line) and $N = 3$ (violet line). (f) Populations of the first six ($n = 2, \dots, 7$) electron excited states $\sum_{l=1}^{n-1} |\alpha_{n,l}(t)|^2$ within a half-cycle of the driver field calculated for $\lambda_0 = 0.8 \mu\text{m}$ and $I_0 = 200$ TW/cm² using the TDSE (solid lines) and the modified SFA of Eqs. (4) and (5) with $N = 3$ (dashed lines).

driver intensities from 30 to 200 TW/cm², the photoionization yield predicted by the single-bound-state SFA is an order of magnitude lower than the photoionization yield in TDSE simulations [see Figs. 2(c) and 2(d)].

We will show now that the dynamics of the electron wave function on the field-subcycle time scale is the key to understanding the difference in the predictions of a single-bound-state model and TDSE. The maps of the probability density $|r\psi(\vec{r}, t)|^2$ calculated using the TDSE and the single-bound-state model of Eq. (2) are shown in Figs. 3(a) and 3(b), respectively. The one-dimensional cuts of these maps along the z axis are presented in Figs. 3(c) and 3(d). The difference in the subcycle quantum dynamics predicted by the TDSE and the single-bound-state SFA model is striking. As can be seen in Figs. 3(a) and 3(b), at the initial phase of the TDSE wave-packet dynamics, the laser field tends to drive the electron wave packet away from the center of the potential well toward the potential barrier, enhancing the right peak of the wave packet [at $t = T_0/8, T_0/4$, and $3T_0/8$ in Fig. 3(c), T_0 being the field cycle], thus increasing the leakage of the electron wave function through the potential barrier. In the single-bound-state SFA model,

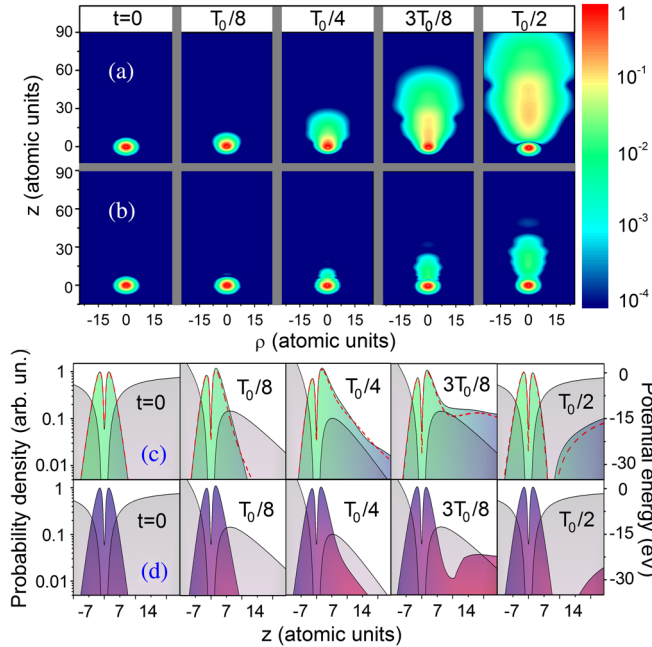


FIG. 3. Spatial maps of the probability density $|r\psi(\vec{r}, t)|^2$ calculated using the TDSE (a) and the single-bound-state SFA model of Eq. (3) (b) for $\lambda_0 = 0.8 \mu\text{m}$ and $I_0 = 200 \text{ TW/cm}^2$ at different instants of time within the field half-cycle. (c), (d) One-dimensional cuts of the probability density calculated using the TDSE (c) and the single-bound-state model of Eq. (2) (d) for $\lambda_0 = 0.8 \mu\text{m}$ and $I_0 = 200 \text{ TW/cm}^2$ at different instants of time measured in units of the field cycle T_0 . The electron wave function calculated with the use of the modified SFA with $N = 3$ is shown by the dashed line. The potential of the atomic core modulated by the driver field is shown by shading.

this effect is, however, much less pronounced [cf. Figs. 3(a) and 3(c) and 3(b) and 3(d)], since the electron wave packet in this model shows little dynamics beyond the spatial profile dictated by the stationary ground-state eigenfunction ψ_0 . As a result, the photoionization yield in this model is much less than the photoionization yield predicted by the TDSE.

TDSE simulations confirm that a high-intensity ultra-short driver pulse indeed efficiently populates excited states [Fig. 2(f)]. The electrons promoted to excited bound states probe a potential barrier of smaller height and width compared to the potential barrier probed by ground-state electrons [Fig. 1(b)]. This opens an additional photoionization pathway, as sketched in Fig. 1(b), which can be much more efficient than photoionization due to direct transitions from the ground state to the continuum [Fig. 1(a)].

The field at which tunneling via excited states starts to dominate photoionization from the ground state can be roughly estimated as the field that suppresses the potential barrier for the first excited bound state, $|E_s| = \pi\epsilon_0 e^{-3} U^{-1}$, where U is the ionization potential of the first excited state. For a hydrogen atom $U = I_p/4$, this estimate gives $|E_s| \approx 2 \times 10^9 \text{ V/m}$, which corresponds to a field intensity $I_s \approx 0.5 \text{ TW/cm}^2$. This estimate agrees well with simulations in Fig. 2(d), where the result calculated with the use of the modified SFA with $N = 2$ starts to noticeably deviate from the single-bound-state SFA photoionization rate for field intensities above 0.5 TW/cm^2 . For argon, $U \approx 4.2 \text{ eV}$, we find $|E_s| \approx 3.1 \times 10^9 \text{ V/m}$ and $I_s \approx 1.3 \text{ TW/cm}^2$.

To quantify the role of excited states, we modify the SFA approach by replacing the ground-state wave function $\psi_0(\vec{r}, t)$ in the definition of $\psi_i(\vec{r}, t)$ in Eq. (2) by an appropriate superposition wave function reflecting the contribution of excited electron states $\psi_b(\vec{r}, t)$. Substituting Eq. (1) into the TDSE $i\hbar\dot{\psi}(\vec{r}, t) = (\hat{H}_0 + \hat{H}_{\text{int}})\psi(\vec{r}, t)$, where \hat{H}_0 is the field-free Hamiltonian and $\hat{H}_{\text{int}} = -eE(t)z$, using a standard SFA assumption that the atomic core has no effect on the continuum states, multiplying the resulting equation by $\psi_{n,l}(\vec{r})$, and integrating it in space, we find that the amplitudes $\alpha_{n,l}(t)$ in this superposition can be found from the equation

$$\hbar \frac{\partial \alpha_{n,l}}{\partial t} = E_n \alpha_{n,l}(t) - eE(t) \sum_{n_1=1}^N \sum_{l_1=0}^{n_1-1} Z_{n_1,l_1}^{n,l} \alpha_{n_1,l_1}(t) - \int_V \psi_{n,l}(\vec{r}) eE(t) z \psi_f(\vec{r}, t) d\vec{r}, \quad (3)$$

where $Z_{n_1,l_1}^{n,l} = \int_V \psi_{n,l}(\vec{r}) z \psi_{n_1,l_1}(\vec{r}) d\vec{r}$.

The continuum population is then written as

$$\tilde{C}(t) = \int |\tilde{a}_p(t)|^2 d\vec{p} = \int \left| \frac{-i}{\hbar} \int_{-\infty}^t \left\{ \int_V \psi_p^*(\vec{r}, t') eE(t') \left[\sum_{n=1}^N \sum_{l=0}^{n-1} \alpha_{n,l}(t') (z\psi_{n,l} - \sum_{n_1=1}^N \sum_{l_1=0}^{n_1-1} z_{n_1,l_1}^{n,l} \psi_{n_1,l_1}) \right] \right\} dt' \right|^2 d\vec{p}. \quad (4)$$

The standard SFA model is recovered by setting $N = 1$ in Eqs. (3) and (4).

As can be seen from Fig. 2(f), the modified SFA model of Eqs. (3) and (4) with $N = 3$ accurately reproduces the results of TDSE simulations for the populations of the electron excited states within a half-cycle of the driver field. The full wave function of an electron in the modified SFA is given by Eq. (1) with $\psi_f(\vec{r}, t) = \int \tilde{a}_p(t) \psi_p(\vec{r}, t) d\vec{p}$. With $N = 3$, this modified SFA wave function, as can be seen from Fig. 3(c), accurately reproduces the results of TDSE calculations for the electron wave packet in a hydrogenlike system driven by a laser field with $I_0 = 200$ TW/cm².

The continuum populations calculated by solving the TDSE and by using the modified SFA approach are compared in Figs. 2(a)–2(c). For low field intensities [$I_0 < 1$ TW/cm²], the contribution of excited states is small. In this regime, the standard, single-bound-state SFA model, which is equivalent to the modified SFA with $N = 1$, provides a reasonable agreement with TDSE simulations [cf. blue and green curves in Figs. 2(a) and 2(d)]. For higher driver intensities [$I_0 > 1$ TW/cm² in Figs. 2(b)–2(e)], populations in excited states are no longer negligible [Fig. 2(f)], and photoionization through excited states becomes significant. In this regime, the standard SFA model fails to accurately describe the continuum population [cf. blue and green curves in Figs. 2(b)–2(e)]. The modified SFA model, on the other hand, can still accurately reproduce TDSE simulations.

For field intensities 1 TW/cm² $< I_0 < 200$ TW/cm², the first excited state, i.e., the state with $n = 2$, acquires the largest population among all the excited states [Fig. 2(f)]. In this range of driver field intensities, the modified SFA model with $N = 2$ provides a reasonably accurate description of $C(t)$ as a function of time and driver intensity I_0 [cf. blue and red curves in Figs. 2(b), 2(d), and 2(e)], which confirms that, in this range of field intensities, of all the excited states, the first excited state ($n = 2$) plays the most significant role in the photoionization process. Moreover, within a broad range of driver intensities, a two-step photoionization [Fig. 1(b)] through this state, as can be seen from Figs. 2(c)–2(e), dominates the overall yield of photoionization.

For driver intensities above 200 TW/cm², predictions of the modified SFA model with $N = 2$ start to noticeably deviate from TDSE results [blue and red curves in Figs. 2(c) and 2(e)], indicating a significant role of photoionization through the second excited state ($n = 3$). Indeed, with this state included in Eqs. (3) and (4), where N should now be taken equal to 3, modified SFA calculations,

as can be seen in Figs. 2(c) and 2(e), agree very well with TDSE simulations.

To directly quantify the contribution of nonadiabatic processes [38,39], the photoionization dynamics was analyzed using the adiabatic representation [40]. The results of these calculations [41] were found to agree very well with the results of TDSE and modified SFA calculations, deviating very significantly from the results of single-state SFA calculations. These findings show that, within the range of parameters considered in this Letter, nonadiabatic transitions can account for no more than a few percent of the discrepancy between the single-state SFA and modified SFA [41].

Direct experimental detection of electron tunneling via excited bound states is challenging, as it requires a time-resolved study of excited-state dynamics on the subcycle time scale. Still, the recently developed laser instruments and methodologies [44,45] could help to confront this challenge. With a few-cycle infrared laser driver inducing ultrafast photoionization in an atomic gas, a subfemtosecond XUV pulse, generated, e.g., using the technology developed in Ref. [46], could serve as an ultrafast probe, transferring transient populations from excited bound states to the continuum, thus giving rise to well-resolved peaks in photoelectron spectra. The amplitudes of these peaks measured as functions of the delay time between the XUV probe and the infrared driver [41] would then reflect the population dynamics of electron excited states.

In summary, we have shown that, in an intense laser field, ultrafast photoionization can occur through quantum pathways that cannot be categorized as multiphoton ionization or ground-state tunneling. In this regime, tunneling from excited electron states can dominate over ground-state tunneling, drastically enhancing photoionization and modifying its dynamics. The modified SFA approach proposed in this work accurately reproduces the predictions of TDSE within a broad range of field intensities. This suggests a convenient way of accurately including excited-state dynamics into models of nonlinear processes in extended media, such as filamentation of ultrashort laser pulses, as well as optical-harmonic and terahertz generation, without the need to solve the TDSE at each point along the propagation path.

This research was supported in part by the Russian Foundation for Basic Research (Projects No. 14-29-07182, No. 16-02-00843, No. 15-02-09370, No. 15-32-20897, and No. 14-29-07201) and the Welch Foundation (Grant No. A-1801). Research into the nonlinear optics in the midinfrared has been supported by the Russian Science Foundation (Project No. 14-12-00772).

- *zheltikov@physics.msu.ru
- [1] L. V. Keldysh, Zh. Eksp. Teor. Fiz. **47**, 1945 (1964).
- [2] M. Lewenstein, P. Balcou, M. Y. Ivanov, A. L'Huillier, and P. B. Corkum, Phys. Rev. A **49**, 2117 (1994).
- [3] A. M. Perelomov, V. S. Popov, and M. V. Terent'ev, Zh. Eksp. Teor. Fiz. **50**, 1393 (1966).
- [4] A. M. Perelomov, V. S. Popov, and M. V. Terent'ev, Zh. Eksp. Teor. Fiz. **52**, 514 (1967).
- [5] M. Ammosov, N. Delone, and V. Krainov, Zh. Eksp. Teor. Fiz. **91**, 2008 (1986).
- [6] N. Bloembergen, IEEE J. Quantum Electron. **10**, 375 (1974).
- [7] M. Lenzner, J. Krüger, S. Sartania, Z. Cheng, C. Spielmann, G. Mourou, W. Kautek, and F. Krausz, Phys. Rev. Lett. **80**, 4076 (1998).
- [8] P. Agostini and L. F. DiMauro, Contemp. Phys. **49**, 179 (2008).
- [9] T. Popmintchev, M.-C. Chen, D. Popmintchev, P. Arpin, S. Brown, S. Ališauskas, G. Andriukaitis, T. Balčiūnas, O. D. Mücke, A. Pugžlys, A. Baltuška, B. Shim, S. E. Schrauth, A. Gaeta, C. Hernández-García, L. Plaja, A. Becker, A. Jaron-Becker, M. M. Murnane, and H. C. Kapteyn, Science **336**, 1287 (2012).
- [10] M. D. Thomson, M. Kieß, T. Löffler, and H. G. Roskos, Laser Photonics Rev. **1**, 349 (2007).
- [11] K. Y. Kim, J. H. Glowia, A. J. Taylor, and G. Rodriguez, Opt. Express **15**, 4577 (2007).
- [12] K. Y. Kim, A. J. Taylor, J. H. Glowia, and G. Rodriguez, Nat. Photonics **2**, 605 (2008).
- [13] A. Couairon and A. Mysyrowicz, Phys. Rep. **441**, 47 (2007).
- [14] L. Bergé, S. Skupin, R. Nuter, J. Kasparian, and J.-P. Wolf, Rep. Prog. Phys. **70**, 1633 (2007).
- [15] P. B. Corkum and F. Krausz, Nat. Phys. **3**, 381 (2007).
- [16] A. Wirth, M. T. Hassan, I. Grguraš, J. Gagnon, A. Moulet, T. T. Luu, S. Pabst, R. Santra, Z. A. Alahmed, A. M. Azzeer, V. S. Yakovlev, V. Pervak, F. Krausz, and E. Goulielmakis, Science **334**, 195 (2011).
- [17] M. Uiberacker, T. Uphues, M. Schultze, A. Verhoef, V. Yakovlev, M. Kling, J. Rauschenberger, N. Kabachnik, H. Schröder, M. Lezius, K. Kompa, H.-G. Müller, M. Vrakking, S. Hendel, U. Kleineberg, U. Heinzmann, M. Drescher, and F. Krausz, Nature (London) **446**, 627 (2007).
- [18] P. Eckle, A. N. Pfeiffer, C. Cirelli, A. Staudte, R. Dörner, H. G. Müller, M. Büttiker, and U. Keller, Science **322**, 1525 (2008).
- [19] H. Akagi, T. Otobe, A. Staudte, A. Shiner, F. Turner, R. Dörner, D. M. Villeneuve, and P. B. Corkum, Science **325**, 1364 (2009).
- [20] M. Schultze, M. Fieß, N. Karpowicz, J. Gagnon, M. Korbman, M. Hofstetter, S. Neppl, A. L. Cavalieri, Y. Komninos, T. Mercouris, C. A. Nicolaides, R. Pazourek, S. Nagele, J. Feist, J. Burgdörfer, A. M. Azzeer, R. Ernstorfer, R. Kienberger, U. Kleineberg, E. Goulielmakis, F. Krausz, and V. S. Yakovlev, Science **328**, 1658 (2010).
- [21] J. Mauritsson, T. Remetter, M. Swoboda, K. Klünder, A. L'Huillier, K. J. Schafer, O. Ghafur, F. Kelkensberg, W. Siu, P. Johnsson, M. J. J. Vrakking, I. Znakovskaya, T. Uphues, S. Zherebtsov, M. F. Kling, F. Lépine, E. Benedetti, F. Ferrari, G. Sansone, and M. Nisoli, Phys. Rev. Lett. **105**, 053001 (2010).
- [22] A. N. Pfeiffer, C. Cirelli, M. Smolarski, D. Dimitrovski, M. Abu-samha, L. B. Madsen, and U. Keller, Nat. Phys. **8**, 76 (2012).
- [23] G. L. Yudin and M. Y. Ivanov, Phys. Rev. A **64**, 013409 (2001).
- [24] E. E. Serebryannikov and A. M. Zheltikov, Phys. Rev. A **90**, 043811 (2014).
- [25] T. Balčiūnas, A. J. Verhoef, A. V. Mitrofanov, G. Fan, E. E. Serebryannikov, M. Y. Ivanov, A. M. Zheltikov, and A. Baltuška, Chem. Phys. **414**, 92 (2013).
- [26] A. J. Verhoef, A. V. Mitrofanov, E. E. Serebryannikov, D. V. Kartashov, A. M. Zheltikov, and A. Baltuška, Phys. Rev. Lett. **104**, 163904 (2010).
- [27] A. V. Mitrofanov, A. J. Verhoef, E. E. Serebryannikov, J. Lumeau, L. Glebov, A. M. Zheltikov, and A. Baltuška, Phys. Rev. Lett. **106**, 147401 (2011).
- [28] B. Yang, K. J. Schafer, B. Walker, K. C. Kulander, P. Agostini, and L. F. DiMauro, Phys. Rev. Lett. **71**, 3770 (1993).
- [29] P. Kaminski, R. Wiehle, V. Renard, A. Kazmierczak, B. Lavorel, O. Faucher, and B. Witzel, Phys. Rev. A **70**, 053413 (2004).
- [30] A. M. Zheltikov and N. I. Koroteev, Phys. Usp. **42**, 321 (1999).
- [31] A. Rudenko, K. Zrost, C. D. Schrter, V. L. B. de Jesus, B. Feuerstein, R. Moshhammer, and J. Ullrich, J. Phys. B **37**, L407 (2004).
- [32] S. Suntsov, D. Abdollahpour, D. G. Papazoglou, and S. Tzortzakis, Phys. Rev. A **81**, 033817 (2010).
- [33] H. Müller, Laser Phys. **9**, 138 (1999).
- [34] M. Nurhuda, A. Suda, and K. Midorikawa, New J. Phys. **10**, 053006 (2008).
- [35] P. Bédot, E. Cormier, E. Hertz, B. Lavorel, J. Kasparian, J.-P. Wolf, and O. Faucher, Phys. Rev. Lett. **110**, 043902 (2013).
- [36] W. Becker, F. Grasbon, R. Kopold, D. Milošević, G. Paulus, and H. Walther, Adv. At. Mol. Opt. Phys. **48**, 35 (2002).
- [37] C. C. Chirilă and R. M. Potvliege, Phys. Rev. A **71**, 021402 (2005).
- [38] H. Nakamura, *Nonadiabatic Transition: Concepts, Basic Theories, and Applications* (World Scientific, Singapore, 2002).
- [39] K. Toyota, O. I. Tolstikhin, T. Morishita, and S. Watanabe, Phys. Rev. Lett. **103**, 153003 (2009).
- [40] A. Karamatskou, S. Pabst, and R. Santra, Phys. Rev. A **87**, 043422 (2013).
- [41] See Supplemental Material at <http://link.aps.org/supplemental/10.1103/PhysRevLett.116.123901>, which includes Refs. [42,43], for the role of nonadiabatic processes and for an outlook for a direct experimental detection of photoionization via excited bound states.
- [42] E. A. Solov'ev, J. Phys. B **38**, R153 (2005).
- [43] C. J. Joachain, N. J. Kylstra, and R. M. Potvliege, *Atoms in Intense Laser Fields* (Cambridge University Press, Cambridge, England, 2012).
- [44] E. Goulielmakis, M. Schultze, M. Hofstetter, V. S. Yakovlev, J. Gagnon, M. Uiberacker, A. L. Aquila, E. M. Gullikson, D. T. Attwood, R. Kienberger, F. Krausz, and U. Kleineberg, Science **320**, 1614 (2008).
- [45] E. Goulielmakis, Z.-H. Loh, A. Wirth, R. Santra, N. Rohringer, V. S. Yakovlev, S. Zherebtsov, T. Pfeifer, A. M. Azzeer, M. F. Kling, S. R. Leone, and F. Krausz, Nature (London) **466**, 739 (2010).
- [46] S. Gilbertson, S. D. Khan, Y. Wu, M. Chini, and Z. Chang, Phys. Rev. Lett. **105**, 093902 (2010).